31st Annual International Conference of the IEEE EMBS
Minneapolis, Minnesota, USA, September 2-6, 2009

An Investigation of Tissue-Temperature Elevation Caused by Recharging of Transcutaneous Nueromodulation Devices

J. Abraham, E. Sparrow, R. Lovik

Abstract—**Heat transfer associated with the electrical recharging of transcutaneous neuromodulation devices was investigated by a combination of experimentation and numerical simulation. The investigation was performed for the most commonly used neuromodulation systems. Temperature elevations within perfused tissue were obtained. For one selected device, it is shown that temperature elevations are sufficiently moderate so as not to cause concern of injury.**

I. Introduction

Biomedical implants frequently experience evolutionary development to improve their functionality and safety. On the other hand, since the changes are driven by functionality, undesirable side effects may be created or enhanced. This paper is focused on evaluating the thermal side effects of evolved neuromodulation implants and their accompanying power sources.

In previous studies [1, 2], three neuromodulation implants and their accompanying power sources were evaluated with regard to thermal impacts. Each of these devices respectively consists of an implant and a power source, the latter being positioned external to the body in close proximity to the implant. The implant is fitted with a short-lifetime battery which must be periodically recharged. The recharging is accomplished by magnetic coupling between the skin-surface-mounted power supply (*antenna*) and the implant. During the recharging period, both the antenna and the implant generate heat internally. In [1], *in vitro* measurements of the heat generated in the individual components were made in a physical simulation of the actual *in vivo* situation. The information obtained in [1] was subsequently used as input in [2] to determine the temperature rise in the tissue adjacent to the implant. These evaluations were performed for the three most commonly used neuromodulation systems.

In the time that has passed since the initial studies [1, 2] were performed, all three of the systems have undergone a significant upgrading. To the best knowledge of the authors, these alterations were made without consideration of their impact on thermal side effects. This situation has motivated the present work. As will be described shortly, a new *in vitro* experimental facility was designed and fabricated to enable the collection of data of highest accuracy. That facility also provided flexibility to accommodate the different shapes and sizes of the respective implants and antennas. The extremely accurate data served as an input to a numerical model of bioheat transfer in the human body. This numerically predicted temperature elevations in the neighborhood of the implant served to indicate the presence or absence of tissue necrosis or discomfort.

Manuscript received April 23, 2009. This work was supported in part by Medtronic Corporation. Ryan Lovik and Eph Sparrow are at the University of Minnesota, Minneapolis, MN 55455-0111.

Corresponding author, John Abraham is at the University of St. Thomas in St. Paul, MN 55105-1079 (e-mail: jpabraham@stthomas.edu).

II. *In Vitro* Physical Model

The features of the *in vivo* situation guided the design of the *in vitro* apparatus. The essential features that had to be included in the design are: (a) the magnetic coupling of the antenna and the implant across a separation distance of 1 cm without attenuation, (b) a means for absorbing the heat energy generated internally in the antenna and in the implant, (c) a containment structure to house and position the antenna and implant, and (d) instrumentation for measuring temperatures. It was found expedient to measure the respective heat generations in the implant and in the antenna in separate experiments rather than in a single experiment. It was decided that these experimental measurements of heat generation would be more accurately determined by experiment rather than by an electromagnetic simulation.

The experimental method is based on the use of a calorimetric fluid which absorbs energy imparted to it by an object whose heat generation rate is to be determined. In the present instance, the heat-generating object is either the antenna or the implant, and the calorimetric fluid is deionized water. The heat-generating object is positioned in the calorimetric fluid, and the timewise temperature rise of the fluid is measured by an array of temperature sensors. The calorimetric fluid has to be housed in a rigid container which is either insulated or is fabricated from an insulating material. The positioning of the implant in the calorimetric cavity was accomplished by the use of four mini-columns which extended upward from the bottom of the recess.

An exploded view of the apparatus is presented in Fig. 1. As seen there, the facility consists of three parts, all of which are fabricated from extruded polystyrene. The lower portion contains a recess which, when the experiment is in progress, contains the calorimetric fluid and the device whose heat generation is to be evaluated. The intermediate portion is a fence-like insert which, upon assembly, fits tightly into the aforementioned cavity. The functions of this insert are

twofold: (a) to define the volume of the calorimetric bath and to allow for implants of various sizes and (b) to provide a means for anchoring and positioning the temperature sensors. The upper part of the apparatus serves as a closure for the calorimetric bath and as an attachment hub for some of the temperature sensors. Note that the upper part of the assembly is fitted with a downward-facing extension which fits into the cavity in the lower portion and serves as an upper bound of the calorimetric fluid.

The relevant dimensions of the apparatus are: (a) basic thickness of the foam slab 38 mm (1.5 in.), (b) depth of the cavity 28.83 mm (1.135 in.), (c) planform dimensions of the recess 102 x 103 mm (4 x 4 in.), (d) thickness of the fence-like structure 12.7 mm (0.5 in.), (e) thickness of the down-facing hub 6.25 mm (0.25 in.), and (f) planform dimensions of the entire apparatus 25.4 x 25.4 mm (10 x 10 in.).

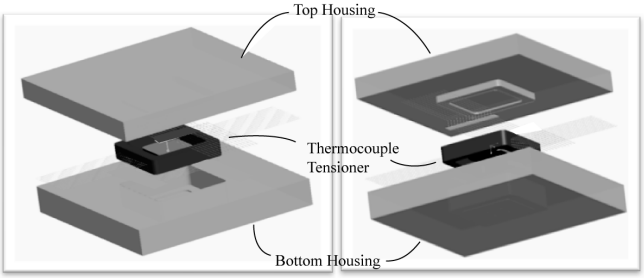

Fig. 1. Schematic diagrams of the components of the experimental apparatus shown in two views.

To obtain highly accurate information about the time-varying temperature distribution within the calorimetric bath, a large number of temperature sensors were distributed throughout the fluid. All told, 30 such sensors were deployed. In addition, one sensor was installed on the external surface of the lower member of the apparatus. Another sensor was positioned in the air just above the upper member but away from any possible interaction with the heating which occurred during the operation of the experiment. Two other sensors were threaded into the bulk of the foam at locations that are 12.7 mm (0.5 in.) and 19 mm (0.75 in.) from the foam-fluid interface.

The temperature sensors were fabricated from 0.075-mm-diameter (0.003 in.) chromel and constantan thermocouple wires. Each thermocouple was formed so that the wires formed a collinear geometry. The use of the collinear geometry resulted in a compact configuration relative to the more conventional "V" thermocouple geometry. The thermocouples were stretched tightly across the calorimetric cavity and were anchored either by the insert or by the downward-extending cap of the cavity.

The first step in the experimental procedure was to establish equilibrium throughout the entire apparatus. A data run was initiated by activating the recharge function of the antenna-implant system. Typically, the duration of a data run extended for at least one hour. During this period, the temperature sensors were sampled continuously with each sensor being visited every 20 seconds. For each of the devices, at least three replicate data runs were performed.

III. Post-processing of the Experimental Data

A. Energy Absorbed in the Calorimetric Fluid

Figure 2 illustrates the traces of the timewise temperature variations at a subset of seven thermocouples out of the array of 30. The selection of thermocouples was taken from various locations within the calorimeter which are intended to convey an important experimental trend. As seen in the figure, two different modes of operation are evident. At early times, there is a startup transient which gives way after about 500 seconds to a regime characterized by a linear increase of the temperature with time at all locations. It is reasonable to regard the latter mode as indicative of quasi-steady operation. The regime of major interest here is the quasi-steady one. In the quasi-steady regime, the heat leaving the heat-generating object (either the implant or the antenna) is steady. Consequently, the slope of the temperature versus time curves provides the rate at which heat from the object enters the surrounding medium.

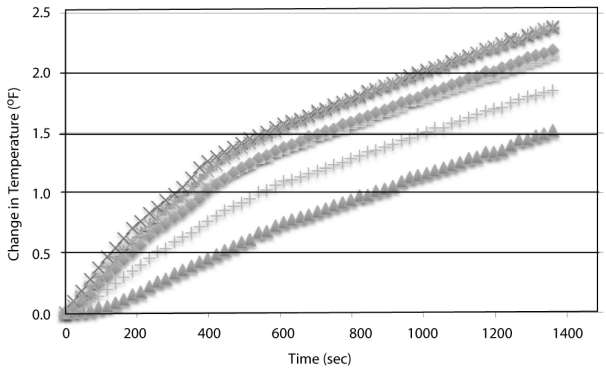

Fig. 2. Representative timewise variations of temperatures measured at various sites within the calorimetric bath.

It was recognized that the heat leaving the object and flowing into the surrounding medium is not uniformly distributed over all the surfaces of the object. For the antenna, the interior geometry of this component was modeled numerically to high resolution so that the surface distribution of the heat flux was obtained as an outcome. On the other hand, only a single specimen of each type of implant was available and could not be sacrificed by opening it to expose its internal geometry. As a consequence, the surface distribution of the leaving heat flow had to be determined in separate experiments. In those experiments, the implant was suspended vertically in an air environment and shrouded with vertical baffles open at the top and bottom. The function of the baffles was to shield the suspended implant from random air currents.

A heat flux meter was adhered to each of the principal faces. Once steady state had been established, the flux meters were read and the respective rates of heat transfer determined from a calibration specification. It was found that the rate of heat transfer from the normally upward-facing surface was substantially greater than that at the

downward-facing surface. For example, for one of the implants (Medtronic Restore Ultra), 70% of the total heat transfer from the implant occurred at the skin-facing surface and 30% was transferred at the other surface.

B. Energy Absorbed in the Foam Housing

In the foregoing, information was conveyed about the energy absorbed in the calorimetric fluid. However, despite the excellent insulating qualities of the foam housing, some energy was absorbed there. To enable the determination of this energy, a numerical simulation model was created and implemented.

Although the system to be modeled is not precisely axisymmetric, an axisymmetric model was created to facilitate the simulation. From past experience, it is expected that the error incurred by utilizing an axisymmetric geometry are negligible. A schematic diagram of the axisymmetric model is illustrated Fig. 3. The diagram shows the implant surrounded by the calorimetric fluid which, in turn, is enveloped by the foam insulation (housing).

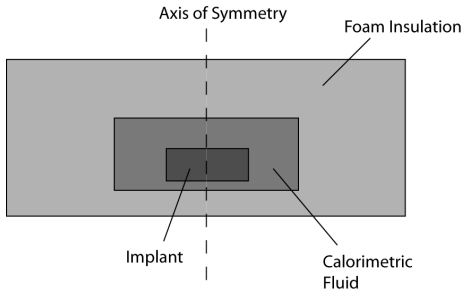

Fig. 3. Axisymmetric model for the numerical simulation.

The solution domain consists of the fluid and the housing. The surface of the implant defines the inner boundary of the solution domain. This model, which excludes the implant from direct participation in the solution, requires that a thermal boundary condition (uniform heat flux) be prescribed at the interface between the implant surface and the calorimetric fluid. The thermal boundary condition at the external surface of the solution domain is convection.

It is assumed that the mode of thermal transport in the solution domain is unsteady heat conduction. For each of the two regions which are in the solution domain, the first law of thermodynamics leads to

$$(\rho c)_i \frac{\partial T_i}{\partial t} = k_i \left[\frac{\partial^2 T_i}{\partial x^2} + \frac{1}{r}\frac{\partial}{\partial r}\left(r \frac{\partial T_i}{\partial r} \right) \right] \quad (1)$$

where i may denote either the calorimetric fluid or the foam housing. In this equation, the quantities ρ, c, and k are, respectively, the density, specific heat, and the thermal conductivity. At all interfaces between the calorimetric fluid and the foam housing, continuity of temperature and heat flux is required. To complete the specification of the problem, the boundary condition at the external surface of the foam housing combines both natural convection and thermal radiation.

The results of the numerical solution showed that the energy absorbed in the foam housing was approximately 3.5% of that absorbed by the calorimetric fluid. This additional energy absorption was accounted for in the *in vivo* numerical simulation which will now be described.

From these determinations, it was found that the rate at which heat passes from the implant and the antenna to their surroundings are 253 and 395 mW, respectively, for the Medtronic Restore Ultra. In contrast, the earlier version of the Medtronic device, the Restore, had corresponding values of 233 and 200 mW. Similar results, although higher heating rates were obtained for the other two commonly encountered nueromodulation devices.

IV. *IN VIVO* THERMAL SIMULATION

An important part of this work is the determination of temperatures of tissue in the near neighborhood of the implant. The solution domain for this study is illustrated in Fig. 4. The implant is situated beneath the skin surface at a depth of 10 mm (0.4 in.). The antenna is aligned with the axis of the implant and is in direct contact with the skin surface.

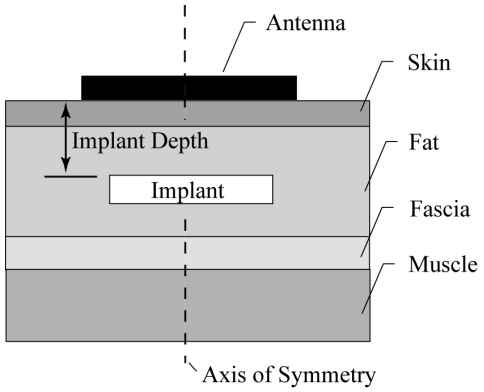

Fig. 4. Solution domain for the numerical simulation of the *in vivo* situation.

Thermal events in the living tissue beds are most commonly modeled by the Pennes bioheat equation [3]. For the axisymmetric geometry considered here, the Pennes equation is

$$(\rho c)_t \frac{\partial T_t}{\partial t} = k_t \left[\frac{\partial^2 T_t}{\partial x^2} + \frac{1}{r}\frac{\partial}{\partial r}\left(r \frac{\partial T_t}{\partial r} \right) \right] + \omega \rho_b c_b (T_a - T_t) + \dot{Q}_{gen} \quad (2)$$

The properties ρ_t, c_t, k_t,ρ_b, and c_b were evaluated at the generally accepted values. The perfusion rate □ was specified to be 0.0018, 0.00043, 0.00043, and 0.0005 (1/s), in the skin, fascia, fat, and muscle, respectively. Correspondingly, values of the volumetric metabolic heat generation rates $\dot{Q}_{gen}$ are 1300, 250, 250, and 500 W/m^3. The solutions were carried out using the finite element computational method. Time step and mesh sizes were small enough to guarantee solutions that were independent of the discretization.

Space limitations preclude the presentation of results for all three of the investigated devices. Here, results will be conveyed for the Medtronic Restore Ultra system. Temperature contour diagrams are displayed in Figs. 5-8 for recharging durations of one and two hours and for two distinct boundary conditions at the exposed surface. One of these conditions corresponds to convective-radiative heat transfer to a room-temperature environment (Figs. 5 and 6). The other pertains to a situation in which the exposed surface interfaces with a highly insulating medium such as a bed or a couch (Figs. 7 and 8). The grey tones have a common scale of temperature in degrees Celsius for all of the four figures.

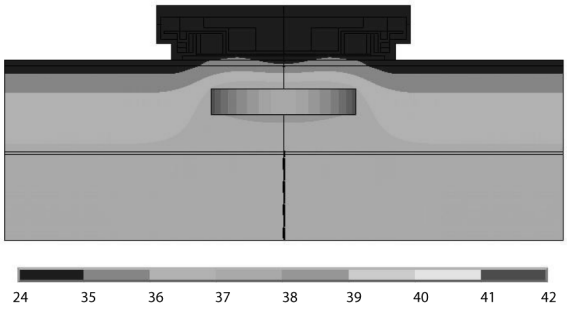

Fig. 5. Temperature contour diagram for one-hour heating in a convective-radiative environment.

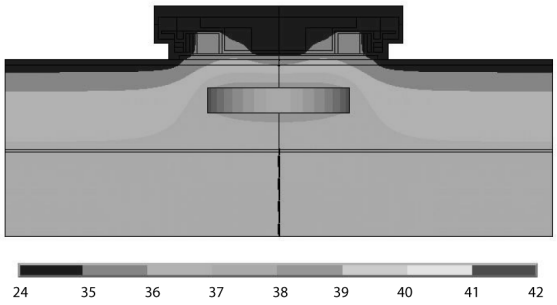

Fig. 6. Temperature contour diagram for two-hour heating in a convective-radiative environment.

Inspection of Figs. 5 and 6 reveals that, for the most part, the tissue temperatures are below the normothermic temperature (37 ^{o}C). Only in the immediate neighborhood of the implant are temperatures as high as 38.5 ^{o}C in evidence. At this temperature level, there is no probability of tissue damage nor is there concern about comfort. These values are for the Medtronic Restore Ultra. For the preceding device, the Restore, the corresponding temperature values are 39.2 and 39.2 ^{o}C. These results are, at first glance, unexpected because the Restore Ultra produces a higher rate of heating compared to the Restore. These results are explained by the fact that the Restore Ultra delivers a greater portion of its heat out the top surface whereas the Restore preferentially emits heat from its bottom surface. These differing heat distributions give rise to the lower temperature levels for the Restore Ultra after one hour of heating in a convective environment.

The situation in which the external surface is insulated shows somewhat higher temperatures which range from 39.2 to 41.4 ^{o}C respectively for one- and two-hour heating durations. The comparison numbers for the Restore are 39.2 and 39.2 ^{o}C.

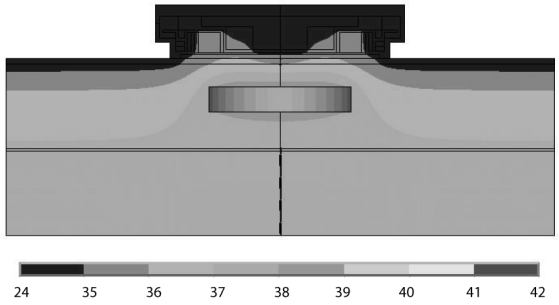

Fig. 7. Temperature contour diagram for one-hour heating in an insulating environment.

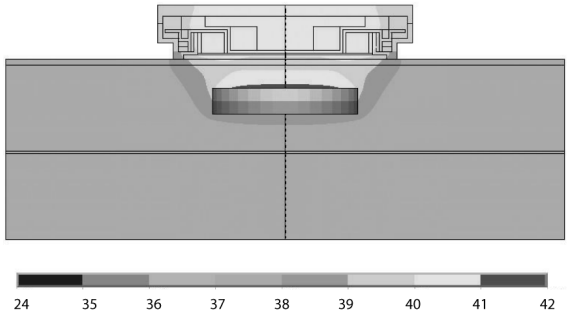

Fig. 8. Temperature contour diagram for two-hour heating in an insulating environment.

V. CONCLUDING REMARKS

Although the Restore Ultra represents a major forward step in functionality, its thermal side effects are somewhat magnified compared to its predecessor, the Restore. However, the somewhat higher temperatures associated with the Restore Ultra are far below those which can cause tissue damage.

REFERENCES

[1] J. J. Weinmann and E. M. Sparrow, "Heat flow from neuromodulation systems into surrounding media," *Neuromodulation*, Vol. 12, no. 2, pp., 114-121, 2009.

[2] R. D. Lovik, J. P. Abraham, and E. M. Sparrow, "Potential Tissue Damage from Transcutaneous Recharge of Neuromodulation Implants", *Int. J. Heat and Mass Transfer*, Vol. 52, pp. 3518-3524, 2009.

[3] H.H. Pennes, "Analysis of tissue and arterial blood temperatures in the resting human forearm," *J. Applied Physiology*, Vol. 85, pp. 5-34, 1948.